Structure and thermodynamics in polymer blends. Neutron scattering measurements on blends of poly(methyl methacrylate) and poly(styrene-*co*-acrylonitrile)

K. Hahn and B. J. Schmitt
BASF Aktiengesellschaft, D-6700 Ludwigshafen, Germany

and M. Kirschey*, R. G. Kirste† and H. Salié
Institut für Physikalische Chemie der Universität Mainz, Germany

and S. Schmitt-Strecker
Max Planck Institut für Chemie, 6500 Mainz, Germany
(Received 26 November 1991; revised 27 March 1992; accepted 27 March 1992)

Neutron scattering on polymer blends of deutero-poly(methyl methacrylate) (D-PMMA) and poly(styrene-*co*-acrylonitrile) with 19 wt% acrylonitrile (PSAN-19) exhibits excess scattering for scattering vectors $Q \lesssim 0.2\,\mathrm{nm}^{-1}$ if the volume fraction of D-PMMA is less than 0.5 and greater than 0.05. The range of occurrence and the amount of excess scattering depends to a certain degree on the procedure of sample preparation. If the excess scattering is eliminated by linear extrapolation from large to small Q in the Zimm representation, the residual scattering intensity in the small and intermediate Q-range can be interpreted by the mean field approach of de Gennes with a concentration-dependent effective interaction parameter. The scattering intensity in the intermediate Q-range can be described with the coil scattering function of Debye using effective radii of gyration and interaction parameters obtained from $Q \to 0$ extrapolated scattering data. In the intermediate Q-range the scattering curves of D-PMMA in the bulk and in the investigated blends show small differences outside the limits of experimental error. These differences are interpreted as an environmental influence of the conformation of the PMMA chain.

(Keywords: structure; thermodynamics; polymer blends; neutron scattering)

INTRODUCTION

In previous papers[1–3] neutron scattering measurements were used in the investigation of polymer blends. In these studies one of the components was present in the dilute state so that the evaluation of the scattering data could be performed according to the well established theory of scattering by dilute systems. On the other hand our knowledge of blends in which both components are present in the concentrated state was based on extrapolating from measurements of the dilute state, with the consequent poor reliability of such conclusions.

In this paper we give measurements on binary polymer blends in which both components are present in the concentrated or semidilute state.

THEORETICAL BACKGROUND

General considerations

In order to describe the scattering intensity of binary polymer mixtures where the two components have different monomer volumes, v_A and v_B, we subdivide the scattering volume into small cells (scattering units) of volume v_0. v_0 can be considered to be the volume of the unit cell of a reference lattice. It is assumed that the chains of both components can be incorporated into this lattice despite the different spatial requirements of their monomer units. It is further assumed that each lattice cell is occupied by one 'monomer unit' of a new kind: its volume is v_0 irrespective of whether it belongs to polymer A or B. This implies further that the mixtures are considered to be incompressible. We define dimensionless concentration functions, $\Phi_i(\vec{X})$, which give the average number of monomers of species i on lattice site $\vec{X}$. The average value of $\Phi_i(\vec{X})$ will be given by the volume fraction of component i but there will be local deviations, $\Delta\Phi_i(\vec{X})$, from this average.

According to the incompressibility assumption (each lattice site is occupied by one monomer unit) the following relation holds for the sum of both concentration functions:

$$\Phi_A(\vec{X}) + \Phi_B(\vec{X}) = 1$$

For such a system the coherent differential cross-section $(d\Sigma/d\Omega)(Q)$ per unit volume is given by[4]:

$$\frac{d\Sigma}{d\Omega}(Q) = 1/v_0\left(b_A\frac{v_0}{v_A} - b_B\frac{v_0}{v_B}\right)^2 S(Q) \qquad (1a)$$

with the structure factor

$$S(Q) = (N^{-1})\langle\Phi_A(\vec{Q})\Phi_A(-\vec{Q})\rangle = (N^{-1})\langle\Phi_B(\vec{Q})\Phi_B(-\vec{Q})\rangle$$

* New address: Degussa AG, Postfach 1345, D-6450 Hanau, Germany
† To whom correspondence should be addressed

0032-3861/92/245150-17

$Q=(4\pi/\lambda)\sin(\vartheta/2)$ is the absolute value of the scattering vector, where ϑ is the scattering angle and λ is the neutron wavelength. $\Phi_i(\vec{Q})$ is the Fourier transform of the concentration function $\Phi_i(\vec{X})$; the angular brackets denote a thermal and spatial average. $b_i v_0/v_i$ is the scattering length of a unit cell occupied by a monomer unit i, where b_i is the scattering length of a monomer unit i. The quotient v_0/v_i takes into consideration the different monomer volumes. N is the number of lattice cells in the scattering volume.

With the contrast factor $K=(b_A/v_A-b_B/v_B)^2$, equation (1a) can be rewritten in a more familiar form:

$$\frac{d\Sigma}{d\Omega}(Q)=v_0 K S(Q) \tag{1b}$$

$S(Q)$ can be considered to be the scattering power per lattice cell. The structure factor $S(Q)$ describes the concentration fluctuations in a homogeneous incompressible polymer blend of components A and B. As has been shown by de Gennes using the mean field random phase approximation, $S(Q)$ is given by the following relation[4,5]:

$$S(Q)^{-1}=1/[\Phi\langle N_A^*\rangle_w P_A(Q)] + 1/[(1-\Phi)\langle N_B^*\rangle_w P_B(Q)]-2\Gamma(\Phi,T) \tag{2}$$

where Φ is the volume fraction of component A, $\langle N_i^*\rangle_w=\langle N_i\rangle_w v_i/v_0$ is the mass average polymerization degree of component i expressed in number of lattice sites occupied. N_i is the usual polymerization degree. $P_i(Q)$ is the form factor of the unperturbed chains of component $i(P_i(0)=1)$.

The generalized Flory–Huggins parameter $\Gamma(\Phi,T)$ in equation (2) accounts for the thermodynamic interactions per unit volume v_0 between the segments A and B. If Γ is independent of Φ, it is identical to the Flory–Huggins parameter χ. However, as we are specifically interested in a possible Φ-dependence of χ, we consider the more general case of a Φ-dependent Flory–Huggins parameter. With the general thermodynamic theorem $S^{-1}(0)=\partial^2\Delta G_m/\partial\Phi^2$ between the scattering function $S(Q)$ for $Q\to 0$ and the Gibbs free energy G_m of mixing per lattice site, which in the Flory–Huggins model[4,6] is given by:

$$\frac{\Delta G_m}{k_B T}=\frac{\Phi}{\langle N_A^*\rangle_w}\ln\Phi+\frac{1-\Phi}{\langle N_B^*\rangle_w}\ln(1-\Phi)+\Phi(1-\Phi)\chi(\Phi) \tag{3a}$$

one obtains for $\Gamma(\Phi)$:

$$\Gamma(\Phi)=-\tfrac{1}{2}\partial^2[\Phi(1-\Phi)\chi]/\partial\Phi^2 = \chi(\Phi)-(1-2\Phi)\frac{\partial\chi}{\partial\Phi}-\tfrac{1}{2}\Phi(1-\Phi)\frac{\partial^2\chi}{\partial\Phi^2} \tag{3b}$$

S(Q) *at small* Q *values*

For small Q values the form factor $P_i(Q)$ can be approximated by:

$$P_i(Q)=1+\tfrac{1}{3}\langle R_{gi}^2\rangle_z Q^2 \tag{4}$$

where $\langle R_{gi}^2\rangle_z$ is the z-average square radius of gyration of component i. Inserting equation (4) into equation (2), $S(Q)$ can be rewritten:

$$\frac{\Phi(1-\Phi)}{S(Q)}=1/\langle\bar{N}\rangle_w(1+\tfrac{1}{3}\langle\bar{R}_g^2\rangle_z Q^2)-2\Phi(1-\Phi)\Gamma(\Phi) \tag{5}$$

where

$$\langle\bar{N}\rangle_w^{-1}=\frac{1-\Phi}{\langle N_A^*\rangle_w}+\frac{\Phi}{\langle N_B^*\rangle_w} \tag{6}$$

$\langle\bar{N}\rangle_w$ is the mass average polymerization degree of the mixture.

$$\langle\bar{R}_g^2\rangle_z=\frac{1}{(1-\Phi)\langle N_B^*\rangle_w+\Phi\langle N_A^*\rangle_w} \times[(1-\Phi)\langle N_B^*\rangle_w\langle R_{gA}^2\rangle_z+\Phi\langle N_A^*\rangle_w\langle R_{gB}^2\rangle_z] \tag{7}$$

is the z-average square radius of gyration of the system.

According to equation (5) one obtains a straight line when plotting the data $\Phi(1-\Phi)/S(Q)$ against Q^2 (the so-called Zimm representation). The slope m of the straight line is given by:

$$m=\langle\bar{R}_g^2\rangle_z/(3\langle\bar{N}\rangle_w) \tag{8}$$

and the intersection with the ordinate by:

$$\Phi(1-\Phi)/S(Q=0)=1/\langle\bar{N}\rangle_w-2\Phi(1-\Phi)\Gamma(\Phi) \tag{9}$$

This means that for known polymerization degrees $\langle N_A^*\rangle_w$ and $\langle N_B^*\rangle_w$ with the aid of equation (6) the z-average radius of gyration $\langle\bar{R}_g^2\rangle_z$ and the generalized Flory–Huggins parameter $\Gamma(\Phi)$ can be determined from the slope and the intersection of the Zimm representation of $S(Q)$.

Q-*dependence of the* Γ-*parameter*

So far we have assumed implicitly that χ is a local interaction parameter and therefore, that the generalized Flory–Huggins parameter Γ in equation (2) is independent of Q. We will now consider the more general situation of a non-local interaction parameter $\chi(r)$. In this case Γ and χ in equations (3) and (5) become Q-dependent. For small Q values $\Gamma(Q)$ can be approximated by[7]:

$$\Gamma(Q,\Phi)=\Gamma(\Phi)[1-\tfrac{1}{6}r_0^2(\Phi)Q^2] \tag{10}$$

where $r_0^2(\Phi)$ is a parameter of the range of interaction. Inserting equation (10) into equation (5) yields:

$$\frac{\Phi(1-\Phi)}{S(Q)}=1/\langle\bar{N}\rangle_w(1+\tfrac{1}{3}\langle\tilde{R}_g^2\rangle Q^2)-2\Phi(1-\Phi)\Gamma(\Phi) \tag{11}$$

where

$$\langle\tilde{R}_g^2\rangle=\langle\bar{R}_g^2\rangle_z+\Phi(1-\Phi)\langle\bar{N}\rangle_w\Gamma(\Phi)r_0^2(\Phi) \tag{12}$$

is the apparent square radius of gyration determined from the slope of the Zimm straight line.

S(Q) *for intermediate* Q *values*

In the intermediate Q-range the small angle approximation of equation (4) no longer holds and the special form of $P(Q)$ has to be taken into consideration. As a first approximation we will use the Debye function to describe the form factors of both chains, although there is experimental and theoretical evidence[8,9] that the form factor of PMMA significantly deviates from the Debye function for $QR_g\gg 1$. In the discussion of the experimental results we will examine the consequences of this assumption in greater detail.

Assuming a Schulz–Flory distribution of the molecular mass the Debye function is given by the following expression[10]:

$$P(Q)=2\frac{\xi-1+(1+U\xi)^{-1/U}}{(U+1)\xi^2} \tag{13}$$

with

$$\xi = \frac{\langle R_g^2 \rangle_z}{1+2U} Q^2 \tag{14}$$

where the non-uniformity $U = (M_w/M_n) - 1$ can be determined by g.p.c. measurements.

For $\xi \gg 1$, $P(Q)$ can be approximated by:

$$P(Q) = \frac{2}{(1+U)(1+\xi)} \tag{15}$$

The validity of this equation depends on U. For $U = 1$ it is the exact representation of equation (13). For very sharp fractions ($U \approx 0$) ξ must be equal to or larger than 10 if the allowed error is 1%. Inserting this approximation into equation (2) and using the same non-uniformity for both components one obtains:

$$\frac{\Phi(1-\Phi)}{S(Q)} = \frac{1+U}{2}\left[\frac{\Phi(1+\xi_B)}{\langle N_B^* \rangle_w} + \frac{(1-\Phi)(1+\xi_A)}{\langle N_A^* \rangle_w}\right] - 2\Phi(1-\Phi)\Gamma \tag{16}$$

Inserting relations (6), (7) and (14) yields:

$$\frac{\Phi(1-\Phi)}{S(Q)} = \frac{1+U}{2\langle \bar{N} \rangle_w}\left(1 + \frac{1}{1+2U}\langle \bar{R}_g^2 \rangle_z Q^2\right) - 2\Phi(1-\Phi)\Gamma \tag{17}$$

With $U = 1$ equation (5) is recovered which in this case is valid in any range of Q.

Equation (17) shows that for similar non-uniformities of both components the coherent scattering intensity at intermediate Q-values ($\xi \gg 1$) can be completely described by the quantities $\langle \bar{N} \rangle_w$, $\langle \bar{R}_g^2 \rangle_z$ and Γ, determined in the small angle regime. In other words, using equation (17) to describe the scattering data at $Q \gg 1/\langle \bar{R}_g \rangle_z$ will allow us to determine the validity of our assumption that the form factors $P_i(Q)$ in equation (2) can be replaced by Debye's function equation (13).

In the preceding papers[1-3] only the low concentration approximation of scattering was considered. As a parameter of thermodynamic interaction the second osmotic virial coefficient A_2 was used. For a small content of component A in the mixture, A_2 is obtained from:

$$\frac{K' c_A}{S(0)} = \frac{1}{\langle M_A \rangle_w} + 2A_2 c_A$$

where c_A is the mass concentration (in g ml^{-1}), M_A is the molar mass of A and K' is a constant. Comparison with equation (2) yields the relation:

$$\lim_{\Phi \to 0} \Gamma = \frac{1}{\langle N_B^* \rangle_w}\left(\tfrac{1}{2} - A_2 v_0 \langle N_B^* \rangle_w \varrho_A^2\right)$$

where ϱ_A is the density of component A. Hence it follows that the χ-values reported in the preceding papers are exactly equivalent to Γ at small or vanishing concentration of one of the components.

EXPERIMENTAL

Synthesis and characterization

Acrylonitrile and styrene were radically polymerized at 142°C and about 9×10^5 Pa in a continuously stirred reactor using ethyl benzene as solvent[11,12]. The product was dried at about 4×10^3 Pa and 200°C, then purified, first by a head-to-tail, then by a sharp precipitation fractionation. The content of acrylonitrile was determined by elementary analysis. The polymer used in this investigation was poly(styrene-*co*-acrylonitrile) containing 19 wt% acrylonitrile (PSAN-19).

To obtain perdeuterated methyl methacrylate (D-PMMA), acetone cyanhydrin was first produced from perdeuterated acetone[13]. The cyanhydrin was dehydrated by concentrated sulphuric acid and esterified with perdeuterated methanol. The deuteration degree of the monomer was determined by n.m.r. to be >98%.

The molecular mass distribution, the different mean values of the molecular masses and the molecular heterogeneity were determined by g.p.c. (*Tables 1* and *2*). The g.p.c. measurements were carried out for pure D-PMMA and pure PSAN-19 in tetrahydrofuran with the freeze-dried polymer foams and with the scattering samples after the annealing procedure which is described below. As can be seen from these data the sample treatment has no influence on the molecular masses and their distributions (*Table 1*).

The molecular masses of D-PMMA and PSAN-19 were further determined by light scattering and viscosimetry, respectively, in butanone. The light scattering measurements were carried out at 25°C. The viscosimetric measurements were made in Ubbelohde-capillary viscometers at 30°C (*Table 2*). The conversion from M_η to M_w has been performed according to the relation[14]:

$$M_\eta = (1-\alpha)(M_n/2) + (1+\alpha)(M_w/2) \tag{18}$$

where α is the exponent of the Mark–Houwink equation.

The tacticity of D-PMMA was investigated by ^{13}C n.m.r. The measurements were carried out by dissolving 80 mg of the substance to be investigated in 2 ml $CDCl_3$. All spectra were recorded at 100.6 Hz. From a comparison of the α-methyl, the quaternary and the carbonyl-C atoms with the corresponding spectra of isotactic, syndiotactic and atactic PMMA, the tacticity of D-PMMA was determined[11,15] (*Table 3*). As these data show, the D-PMMA is highly syndiotactic.

Sample preparation

Weighed amounts of both polymer components and the pure components for the blank samples were

Table 1 Molar mass average M_w and M_n and non-uniformity of the pure polymers before and after sample preparation (including annealing for 3 h at 140°C) as determined by g.p.c.

	M_w (g mol^{-1})		M_n (g mol^{-1})		$U = M_w/M_n - 1$	
Polymer	Before	After	Before	After	Before	After
D-PMMA	224 000	229 000	121 000	124 000	0.85	0.85
PSAN-19	248 000	252 000	127 000	132 000	0.95	0.91

Table 2 Molar mass average M_w determined for the pure polymers with different experimental methods

Polymer	Method	M_w (g mol^{-1})
D-PMMA	g.p.c.	224 000
	Light scattering	226 000
PSAN-19	g.p.c.	248 000
	Viscosimetry	220 000

Table 3 Tacticity of D-PMMA determined by triad analysis of the ^{13}C n.m.r.-signal of the quaternary C atom. For comparison, the compositions of isotactic, syndiotactic and atactic PMMA are also given

Triad	Isotactic PMMA	Atactic PMMA	Syndiotactic PMMA	D-PMMA
Isotactic	0.85_8	0.21_9	0.02_3	0.042
Heterotactic	0.13_7	0.53_1	0.26_1	0.326
Syndiotactic	0.00_3	0.25_0	0.71_6	0.632

dissolved in dioxane at a combined concentration of ~2.5%. The solution was rapidly frozen in a cold mixture of methanol and dry ice and was freeze-dried for about 100 h at increasing temperature (10–50°C).

The polymer foams obtained with this procedure were hot-pressed under vacuum for about 15 min at 170°C at a constant pressure of 16 MPa. The samples were then cooled below the glass transition temperature at a cooling rate of about 5°C min^{-1} and constant pressure. Finally the samples were heated up again to 140°C, annealed for 3 h at this temperature and than quenched in order to freeze-in the chain conformation. During the annealing procedure sufficient pressure was applied to guarantee a constant sample form.

To test the influence of the preparation method on the scattering curves, some of the samples were additionally annealed for either 80 or 500 h at 140°C as well as for 10 h at 160°C and then for another 10 h at 140°C (see *Table 4*).

SANS experiments

SANS experiments were performed using the D11 and D17 small angle diffractometers at the high flux reactor in the Institute Laue-Langevin (ILL), Grenoble, France[16,17]. The D11 measurements were made with a sample-to-detector distance of 10 m and a neutron wavelength of $\lambda = 1.0$ nm ($\Delta\lambda/\lambda = 0.1$). The D17 measurements were carried out at sample-to-detector distances of 3.46 m and 1.4 m using a neutron wavelength of 1.5 nm ($\Delta\lambda/\lambda = 0.1$). This combination provided access to a range of scattering wave vectors of $0.03\ nm^{-1} < Q < 1\ nm^{-1}$. In all cases the neutron beam area at the sample was defined by a 1.2 cm diameter cadmium pinhole. Scattered neutrons were collected on a detector with area 64 cm × 64 cm.

Data evaluation

The two-dimensional scattering data were circularly averaged by ILL-supported routines[18] to obtain the one-dimensional form of scattering intensity *versus* momentum transfer Q. After subtracting the scattering contributions due to empty sample holder and electronic background, the resulting intensities were divided by the transmission factor and the sample volume. The corrections for counter efficiency were made with a water standard of 1 mm thickness. The same water standard was used to carry out the calibration to units of absolute scattering intensity (cm^{-1}).

The total (single and multiple) scattering probability per solid angle from a water sample with thickness D is given by

$$g(\lambda)[1-\exp(-D(d\Sigma/d\Omega)_w]/4\pi$$

where $(d\Sigma/d\Omega)_w$ is the total scattering cross-section of water. The factor $g(\lambda)$ takes into account changes in the detector efficiency for inelastically scattered neutrons. At $\lambda = 1$ nm and 1.5 nm the following g-factors were used[19,20]: $g(1\ nm) = 0.96$, $g(1.5\ nm) = 0.79$.

The background scattering contributions to the total measured scattering intensities of the mixtures have been estimated from the SANS intensities obtained from the blank samples of D-PMMA and PSAN-19. From the Q-independent tail of the scattering curves of the blank samples the incoherent contributions to the scattering intensities of the mixtures were calculated using the methods reported by Hayashi *et al.*[21] and O'Reilly *et al.*[22].

The coherent background scattering contributions were calculated according to Gawrisch *et al.*[23] and Akcasu *et al.*[24], using the relation:

$$I_{coh}(\Phi, Q) = [\Phi\sqrt{I^{coh}_{D\text{-}PMMA}} + (1-\Phi)\sqrt{I^{coh}_{PSAN\text{-}19}}]^2 \quad (19)$$

The coherent scattering intensities of the deuterated and protonated blanks, $I^{coh}(Q)$, are obtained as the difference between the total scattered intensity and the flat incoherent background of the corresponding blank samples. This treatment of the coherent background implicitly assumes that all the samples (blanks and mixtures) have the same forward scattering. The problem of the subtraction of the coherent background is discussed in greater detail in Appendix A.

After the correct subtraction of the background scattering, the remaining reduced scattering intensity per unit volume is given by the differential cross-section defined in equations (1a) and (1b). In order to be able to express $d\Sigma/d\Omega$ in terms of the form factors of two polymeric components A and B, the copolymer PSAN-19 is treated as a homopolymer consisting of average PSAN-19 monomer units. *Table 5* lists the physical properties of the D-PMMA and PSAN-19 monomer units which were used for the data analysis. The scattering length b and the molar mass M of the average PSAN-19 monomer unit have been calculated according to:

$$p(PSAN) = xp(S) + (1-x)p(AN) \quad (20)$$

where p is b or M and $x = 0.689$ is the number fraction of styrene monomers in the average PSAN-19 chain. ϱ has been determined by density measurements[1] at 25°C and v has been calculated from ϱ and M_0 ($v = M_0/\varrho N_0$, where N_0 = Avogadro's number and M_0 = molar mass of the monomer). For a deuteration degree of the D-PMMA monomers of 98% one obtains a contrast factor $K = 2.78 \times 10^{21}\ cm^{-4}$.

As can be seen from the data in *Table 5*, the volumes of the monomer units of the D-PMMA and the average PSAN-19 chain are very similar. This means that the description of both components with the same lattice is well justified for this system. The lattice reference volume

Table 4 Annealing procedure of the samples

Experiment	Procedure
D17 measurements (*Table 7*)	3 h at 140°C or 2 h at 200°C
D11 measurements (*Table 7*)	10 h at 160°C + 10 h at 140°C
Special annealing of the sample with $\Phi = 0.173$	80 h at 140°C or 500 h at 140°C
Special annealing of the sample with $\Phi = 0.358$	80 h at 140°C

Table 5 Physical properties of the D-PMMA and PSAN-19 monomer units used for the data analysis

Polymer	Sum formula	Scattering length, b (10^{-12} cm)	Molar mass, M (g mol^{-1})	Density, ϱ (g cm^{-3})	Volume, V (10^{-22} cm^3)
D-PMMA	$C_5D_8O_2$	9.795	108.17	1.278	1.406
H-PMMA	$C_5H_8O_2$	1.467	100.12	1.183	1.406
PS	C_8H_8	2.296	104.15	1.050	1.646
AN	C_3H_3N	1.801	53.06		
PSAN-19	C_8H_8 (68.9%)+C_3H_3N (31.1%)	2.14	88.26	1.068	1.374

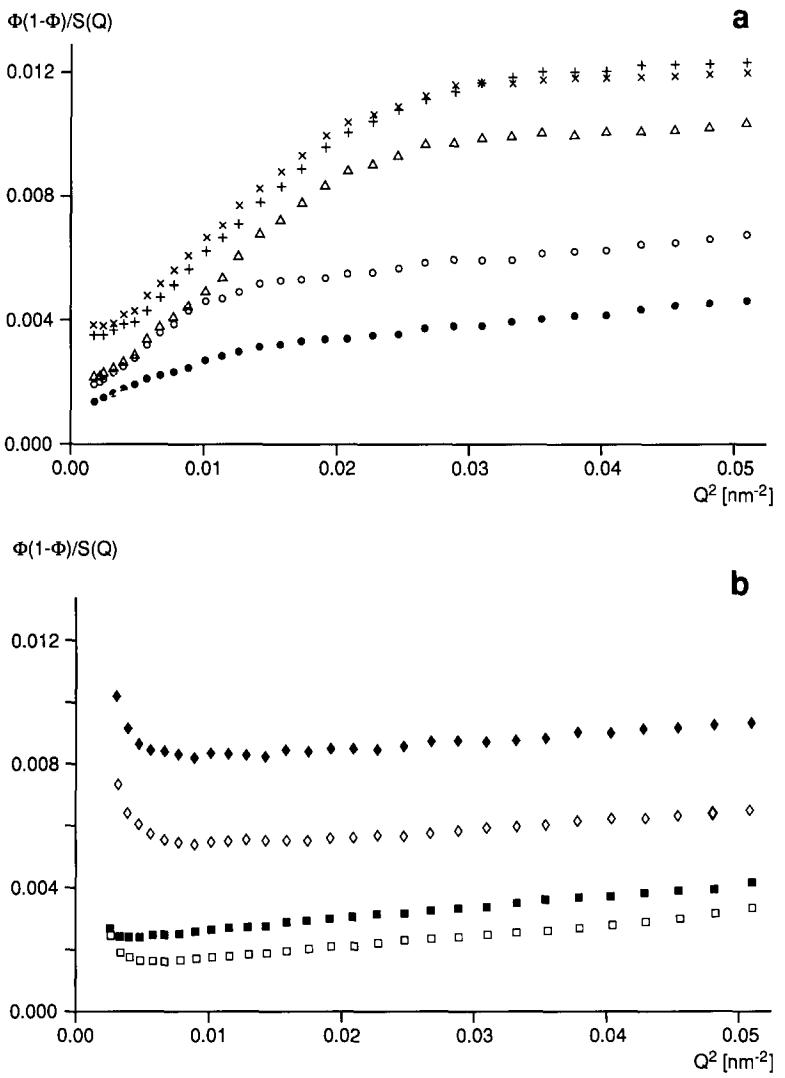

Figure 1 Small angle neutron scattering (SANS) from mixtures of D-PMMA and PSAN-19. Conditions: instrument, D11; sample to detector distance = 10 m; $\lambda = 1.0$ nm; $T = 25$°C. Annealing procedure: 10 h at 160°C plus 10 h at 140°C. Volume fractions of D-PMMA: (a) ●, 0.042; ○, 0.085; △, 0.173; ×, 0.264; +, 0.358. (b) ◆, 0.556; ◇, 0.661; ■, 0.770; □, 0.883

v_0 was chosen as the arithmetic average of the monomer volumes v_A and v_B ($v_0 = 1.393 \times 10^{-22}$ cm^3). This leads to polymerization degrees $\langle N_i^* \rangle_w$ ($\langle N_i^* \rangle_w = M_{iw}/(\varrho_i v_0 N_0)$) of 2120 for D-PMMA and 2630 for PSAN-19.

RESULTS AND DISCUSSION

SANS data

In *Figures 1a* and *b* structure factors $S(Q)/\Phi(1-\Phi)$ of the mixtures are shown in the Zimm representation at small Q-values. A comparison of the figures shows that very different scattering profiles are obtained for volume fractions Φ of D-PMMA less than and greater than 0.5. For Q-values greater than 0.1 nm^{-1} the measured intensities of the samples with $\Phi > 0.5$ (*Figure 1b*) show a straight line behaviour, as one would expect according to equations (5) or (17). However, a totally different and unexpected scattering profile is obtained for the samples containing volume fractions of D-PMMA less than 0.5 (*Figure 1a*). The Zimm representations of these scattering intensities show distinct inflections at Q-values of about 0.2 nm^{-1}, with a stronger decrease of the reciprocal intensities for $Q < 0.2$ nm^{-1}. The $\Phi = 0.455$ mixture of this sample set has an unexpectedly high scattering intensity. A second $\Phi = 0.455$ sample prepared under the same conditions did not exhibit such a high scattering

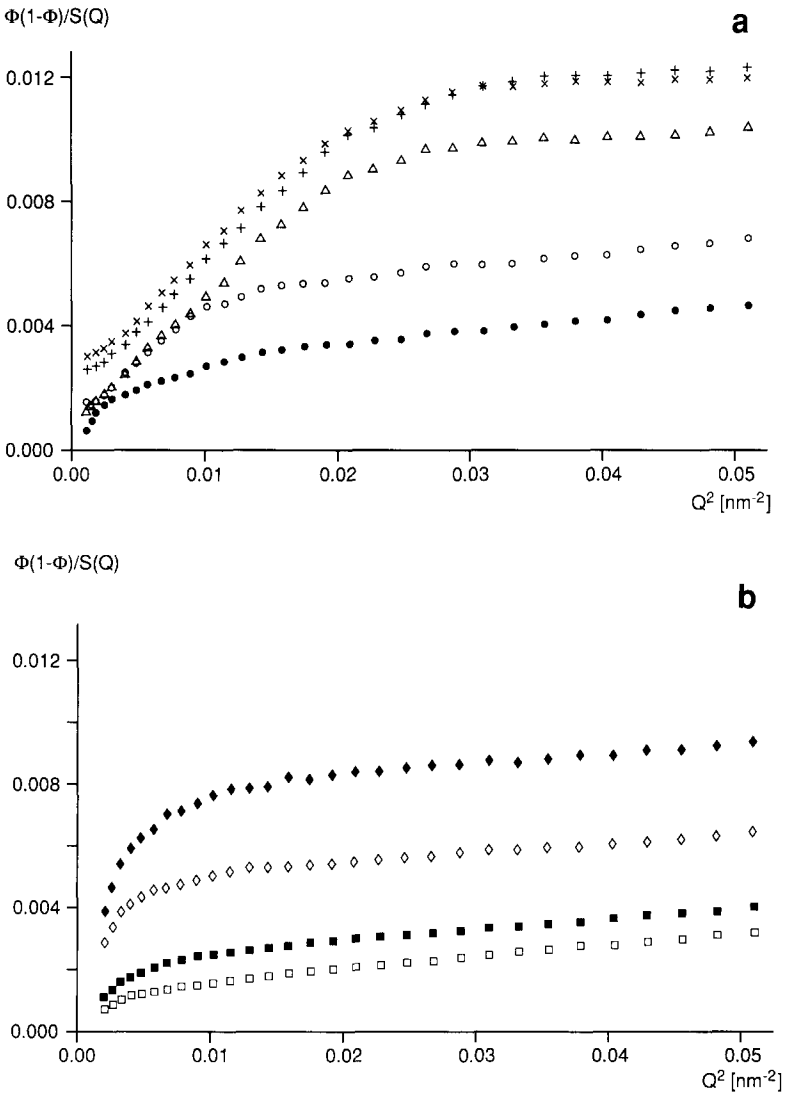

Figure 2 SANS from mixtures of D-PMMA and PSAN-19 as in *Figure 1* but not corrected for coherent background contributions

power. It is not shown in *Figure 1* because a different instrument was used (D17 instead of D11) but it is considered in *Table 7*.

Whenever unusual SANS patterns like those in *Figure 1a* are observed, one has to consider the possibility of an error in subtraction of the coherent background, caused, for example, by microvoid scattering. In *Figure 2a* the scattering intensities of the samples with $\Phi < 0.5$, not corrected for coherent background contributions, are represented in the Zimm form. A comparison of *Figures 1a* and *2a* shows that the subtraction of the coherent background has little effect on the profiles of these scattering data. As a matter of fact some of the scattering curves represented in *Figure 1a* show an increase of the reciprocal intensity at the smallest Q-values, indicating that in this Q-range too much coherent background has been subtracted. However, the effect of background subtraction decreases so rapidly that it has lost any significance for Q-values $> 0.14\,\mathrm{nm}^{-1}$. In particular it has no effect at all on the inflection of the scattering data at about $0.2\,\mathrm{nm}^{-1}$.

On the other hand, the more or less pronounced increase of the reciprocal intensities at the smallest Q-values ($Q < 0.12\,\mathrm{nm}^{-1}$) observed for the samples with $\Phi > 0.5$, is most likely due to a wrong subtraction of the coherent background. This can be seen from a comparison of the scattering data shown in *Figure 1b* with those of *Figure 2b*, where no coherent background has been subtracted. In both cases the deviation from a linear behaviour occurs in the same Q-range ($Q < 0.12\,\mathrm{nm}^{-1}$), but in opposite directions. This indicates that the actual coherent scattering background of the mixtures is smaller than that estimated from the scattering intensities of the blanks according to equation (19). As is clear from this equation, the contrast between the inclusions which cause the coherent background scattering (see Appendix) and the polymer matrix increases quadratically with the volume fraction of the deuterated material. Therefore one expects any error in the background subtraction due to differences in the size distributions of the inclusions in the blanks and the mixtures, to show up much more strongly in the highly deuterated samples.

The inflection observed in the Zimm plots could also indicate that a (partial) demixing of the polymeric components takes place. As all the samples — even after prolonged annealing — were highly translucent, the demixed phases, if they exist, must be of small domain size (significantly smaller than 400 nm). Transmission electron microscopy (TEM) investigations[25] of the mixtures with $\Phi < 0.5$ did not show any evidence for the existence of phase separation on a scale larger than 5 nm. As TEM is sensitive only to strongly demixed phases,

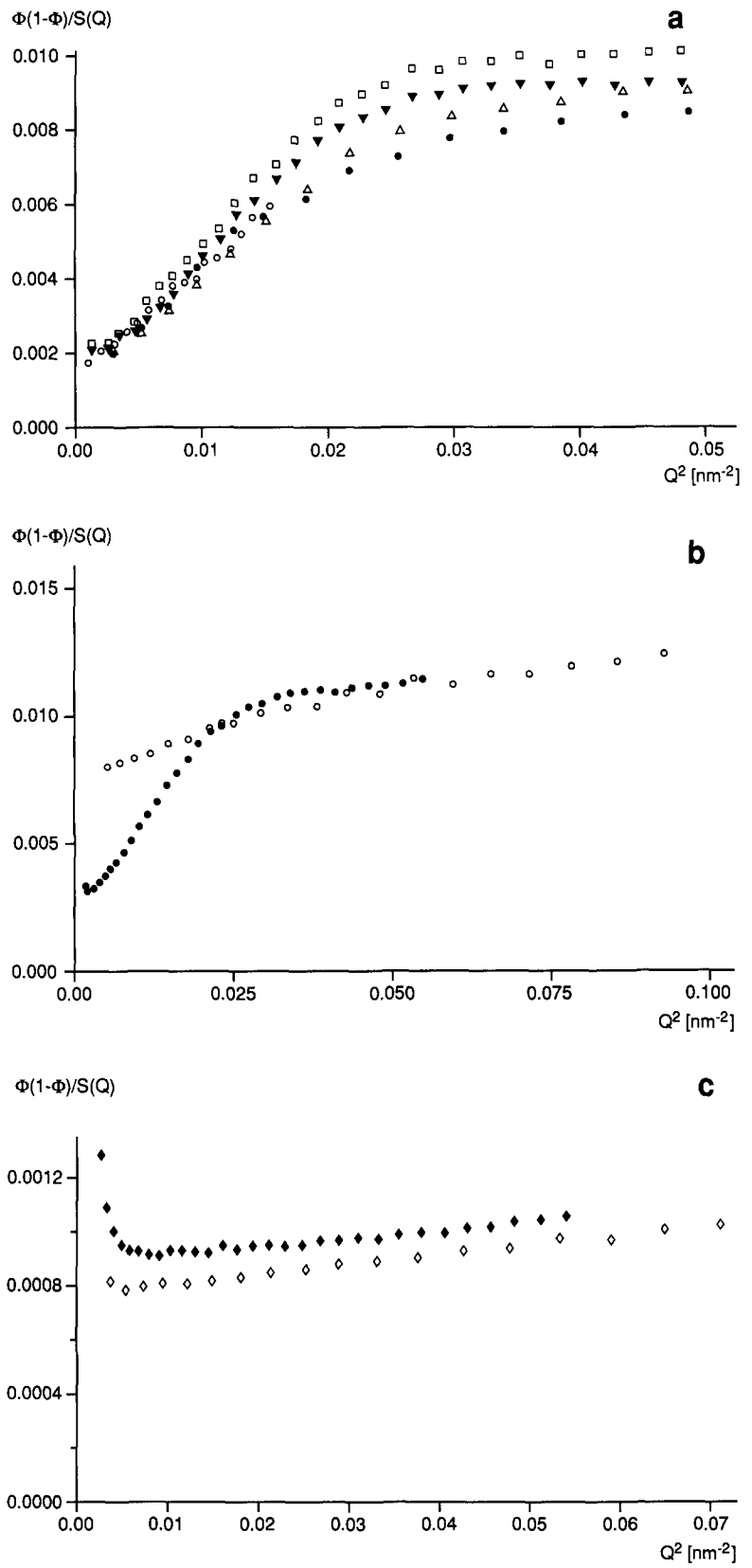

Figure 3 SANS from mixtures of D-PMMA and PSAN-19 showing the dependence of the excess scattering on annealing conditions. Volume fractions of D-PMMA and annealing conditions: (a) $\Phi=0.173$; ●, ○, 3 h at 140°C; △, 80 h at 140°C; ▼, 500 h at 140°C; □, 10 h at 160°C plus 10 h at 140°C. (b) $\Phi=0.358$; ○, 3 h at 140°C; ●, 80 h at 140°C. (c) $\Phi=0.556$; ◇, 3 h at 140°C; ◆, 10 h at 160°C plus 10 h at 140°C

this does not rule out, however, the existence of phases with slightly different compositions.

Further evidence against phase separation is provided by the scattering curves shown in *Figures 1a* and *b*. For all mixtures the extrapolation of the Zimm plots to $Q=0$ yields intersections with the ordinate larger than $1/\langle\bar{N}\rangle_w$. If there were any tendency to phase separation due to the incompatibility of both components, intersections smaller than $1/\langle\bar{N}\rangle_w$ would be expected.

In an attempt to understand the origin of the scattering behaviour of the mixtures with low D-PMMA contents it is also necessary to investigate whether the scattering

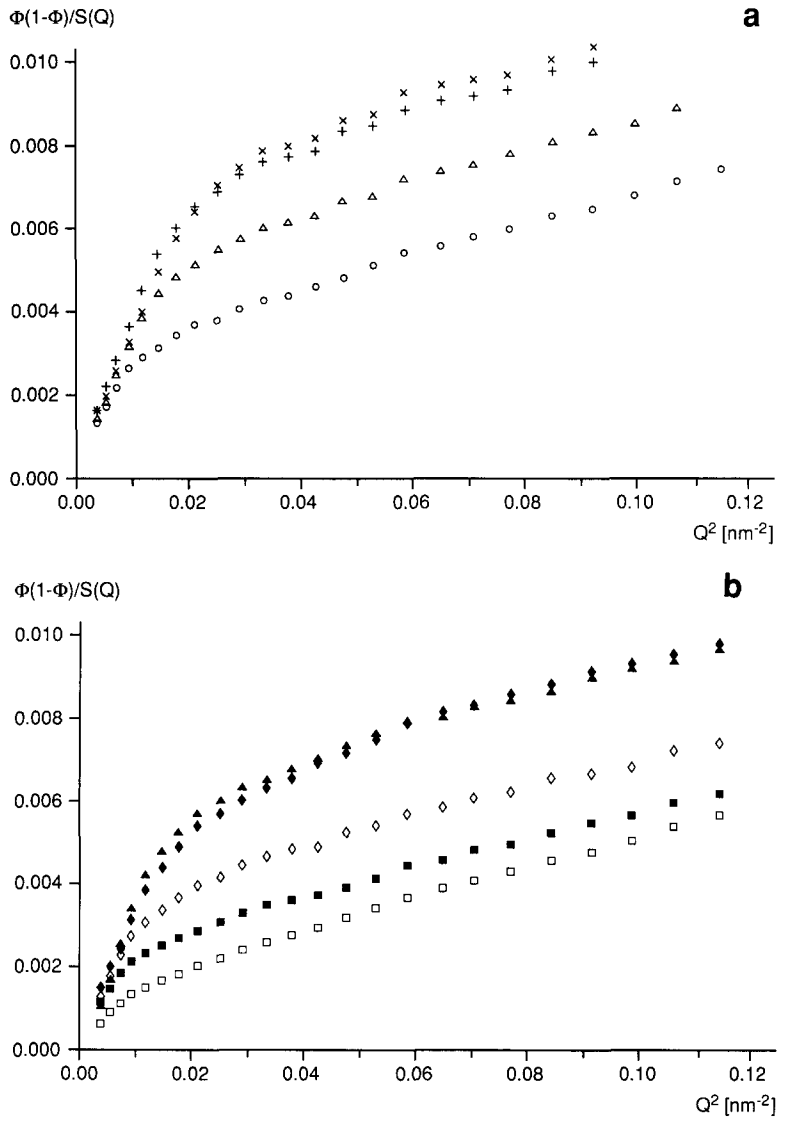

Figure 4 SANS from mixtures of D-PMMA and PSAN-19. Conditions: instrument, D17; sample to detector distance = 3.46 m; $\lambda = 1.5$ nm; $T = 25$°C. Annealing procedure: 2 h at 200°C. Volume fractions of D-PMMA: (a) ○, 0.085; △, 0.173; +, 0.264; ×, 0.358. (b) ▲, 0.455; ◆, 0.556; ◇, 0.661; ■, 0.770; □, 0.883

behaviour is preparation dependent. For this purpose samples with largely different annealing conditions were prepared (see *Table 4*). The effect of the different annealing treatments is shown in *Figures 3a* to *c* for mixtures containing D-PMMA volume fractions of 0.173, 0.358 and 0.556, respectively. For these blends new samples as well as new blanks were prepared for the different annealing conditions.

As *Figure 3a* ($\Phi = 0.173$) demonstrates, the inflection in the scattering curve does not vanish but becomes even more pronounced with increasing annealing time. In *Figure 3b* the Zimm representations of the $\Phi = 0.358$ sample annealed for 3 and 80 h at 140°C are shown. After an annealing time of 3 h only a slight inflection can be observed. With prolonged annealing of the same sample this inflection becomes very pronounced due to a strong increase of the scattering intensity at Q values smaller than 0.17 nm^{-1}. For both volume fractions, the extrapolation of the Zimm plots from the steep part of the curves to $Q = 0$ does not yield intercepts smaller than $1/\langle \bar{N} \rangle_w$. This again shows that the unusual scattering pattern is not due to demixing effects of both polymer components.

For the $\Phi = 0.556$ samples (*Figure 3c*) no significant effect of the annealing time on the scattering behaviour was observed within the experimental accuracy (relative systematic errors about $\pm 4\%$). It is noteworthy that prolonged annealing does not give rise to a bend in the Zimm representation of the scattered intensity for this mixture.

The small angle measurements with D17 were obtained from new samples. With the standard annealing procedure (3 h at 140°C) similar results have been obtained, as shown in *Figures 1a* and *b*. Since the Q-values are somewhat greater, the linear range of the scattering curves is larger and the range of excess scattering is smaller than in *Figure 1*. The $\Phi = 0.455$ mixture exhibited no excess scattering in this experiment.

A more homogeneous scattering behaviour is obtained when the samples are annealed at 200°C (*Figures 4a* and *b*). Clear deviations from a linear profile are observed for all the mixtures, irrespective of the volume fraction of D-PMMA. A comparison of the scattering curves of the samples annealed at 140°C and 200°C shows that the absolute intensities and the slopes of the linear parts of the intensities are also different. In *Figures 5a* and *b* the

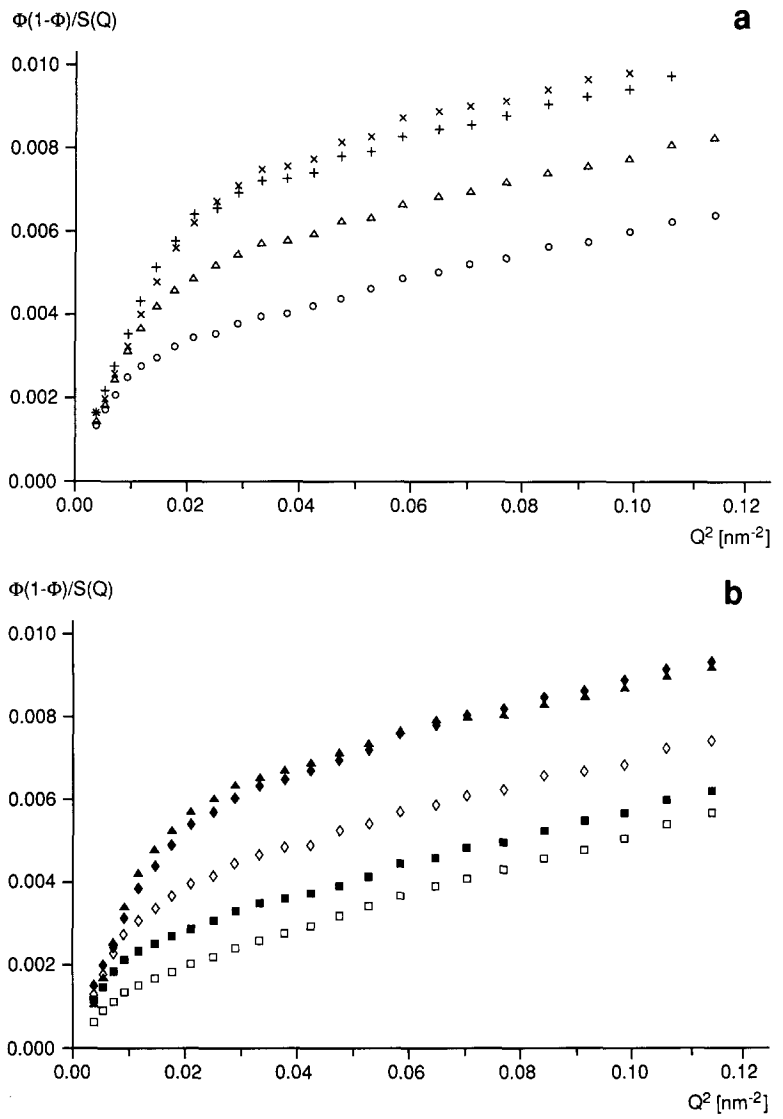

Figure 5 SANS from mixtures of D-PMMA and PSAN-19 as in *Figure 4* but not corrected for background scattering

scattering intensities of the samples annealed at 200°C and not corrected for the coherent background scattering are represented. From a comparison of *Figures 4* and *5* it is obvious that coherent background subtraction has very little effect on the scattering profiles. In particular it has no effect at all on the inflection of the scattering curves.

The discussion on the SANS curves obtained from samples which were annealed at 140°C is not applicable in every respect to the curves in *Figures 4* and *5*. In particular the ordinate intercepts of the curves in *Figures 4* and *5* are so near to zero that in these measurements the formation of larger aggregates cannot be excluded.

Anomalous scattering effects have been repeatedly observed in SANS, X-ray and light scattering investigations on moderately concentrated polymer solutions in good, low molecular mass solvents. Koberstein *et al.*[26] as well as Wendt and Springer[27] described the non-linearity in the Zimm plots in terms of 'excess scattering' contributions, not related to the single chain form factor. No explanation of the physical origin of this excess scattering is given. Dautzenberg[28] explains the anomalous scattering behaviour by the assumption of a molecular network, which is formed as soon as the polymer concentration is sufficiently high for a significant overlapping of the chains to occur. Thus the deviation from a linear form of the Zimm plots is explained by intermolecular, rather than intramolecular, scattering contributions. Schwahn *et al.*[6] obtained no excess scattering in SANS experiments on blends from polystyrene and poly(vinyl methyl ether).

As already mentioned, the scattering data have to be extrapolated to $Q=0$ in order to determine the generalized Flory–Huggins parameter and the radius of gyration. It therefore needs to be clarified whether the extrapolation should be carried out from the steep or the flat part of the Zimm curves. In other words we have to find out if the inflection in the Zimm representations is caused by a special non-Gaussian chain form factor (intramolecular effects) or by non-thermodynamic intermolecular scattering contributions. Only if the whole scattering intensity is due to intramolecular or thermodynamic effects can it be described by equation (2) over the whole Q range. In this case the extrapolation must be carried out from the steep part of the Zimm curves.

In *Table 6* the radius of gyration, R_g, values obtained by fitting a straight line through the measuring points of the steep and flat regions of the Zimm representations are listed. The average degrees of polymerization of the mixtures calculated by equation (6) were used for this purpose. For the $\Phi=0.77$ and 0.883 mixtures annealed

at 200°C no straight line could reasonably be fitted through the measuring points at the smallest Q values. For $\Phi = 0.455$ and 0.556, negative intercepts were obtained. Therefore no R_g value was evaluated for these samples. For all the other samples the extrapolation from the steep part of the Zimm curves yielded very large R_g values. The values are about three times as high as those measured in the diluted systems[3], D-PMMA dissolved in PSAN-19 (16.0 nm) and PSAN-19 dissolved in D-PMMA (17.6 nm, extrapolated z-averages*).

On the other hand all radii of gyration determined by extrapolating the scattering data from the flat part of the Zimm representations are in fairly good agreement with the values measured in the bulk state[2,8] for the single components PMMA (14.8 nm) and PSAN-19 (15.4 nm)*. This is in accordance with the results expected from theoretical considerations[4]. These data indicate with great certainty that the inflection in the Zimm curves is not related to single chain scattering contributions.

To confirm this conclusion further an additional test was carried out by measuring the chain conformation of the D-PMMA molecules in a thermodynamically concentrated but optically dilute system. For this purpose a mixture containing 35 mass% PMMA (1% of which was perdeuterated) and 65% PSAN-19 was prepared according to the usual procedure described above. The protonated sample had a molar mass of 250 000 g mol^{-1} and a tacticity similar to D-PMMA. *Figure 6* shows a comparison of the Zimm representation of the scattering intensities of this sample and the concentrated mixture with $\Phi = 0.358$. Both samples were annealed for about 3 h at 140°C. Totally different scattering curves were obtained. Most important, however, no inflection occurred in the Zimm representation of the optically dilute system. The radius of gyration, $\langle R_g \rangle_z = 14.9$ nm determined from the slope of the straight line, is in good agreement with the value determined in the bulk state[8] (14.8 nm).

According to the above experimental evidence we can conclude that the inflection observed in the Zimm representation is not caused by intramolecular but rather by intermolecular scattering contributions. This means that the radii of gyration and the generalized Flory–Huggins parameters need to be determined by extrapolating the scattering data from the flat part of the Zimm representations, dismissing the data at small Q values. This extrapolation has been performed linearly. Koberstein's extrapolation procedure[26] has been tried but it did not yield the best reproduction of scattering data in any case.

* To aid comparison the radii of gyration from the cited literature were corrected in the following way: The original data were interpolated for matching the molecular weights of the samples in this paper (225 000 for PMMA and 234 000 for PSAN-19). The data were then corrected for the different non-uniformities according to[29]:

$$\langle R_g^2 \rangle_{z,corr} = \langle R_g^2 \rangle_z f(U_1)/f(U_2)$$

with

$$f(U) = \frac{1+2U}{1+U} \frac{\Gamma(1/U+3+\varepsilon)}{\Gamma(1/U+3)} \left(\frac{1}{U}+1\right)^{\varepsilon}$$

The meaning of ε is given by the relation $R_g^2 \propto M^{1+\varepsilon}$. U_1 is the non-uniformity of the samples in this paper (0.85 for PMMA and 0.93 for PSAN-19), U_2 is the non-uniformity of the samples in the cited papers.

Table 6 Radius of gyration, R_g, evaluated from the steep and flat part of the Zimm plots

Annealing condition	Volume fraction, Φ	R_g (nm) (steep part)	R_g (nm) (flat part)
10 h at 160°C	0.085	39	14.6
+10 h at 140°C	0.128	45	13.1
	0.173	47	13.1
	0.264	49	12.2
	0.358	53	12.0
2 h at 200°C	0.085	39	16.1
	0.173	45	16.1
	0.264	50	16.0
	0.358	46	15.8
	0.455	negative intercept	16.1
	0.556	negative intercept	16.7
	0.661	46	16.2
	0.770	–	16.4
	0.883	–	16.7

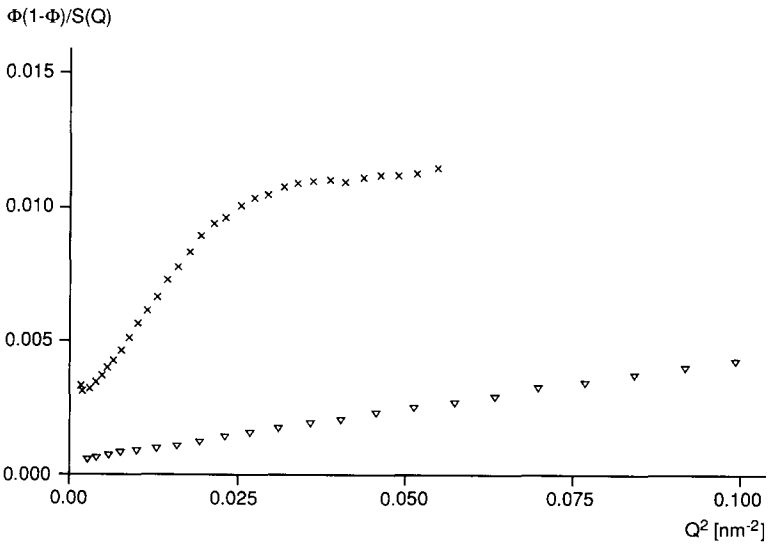

Figure 6 SANS from mixtures of PMMA and PSAN-19. ×, Φ(D-PMMA)=0.358, Φ(PSAN-19)=0.642; ▽, Φ(D-PMMA)=0.0031, Φ(H-PMMA)=0.307, Φ(PSAN-19)=0.690 (optically thin)

Table 7 Radii of gyration $R_g(=\langle \bar{R}_g^2\rangle_z^{1/2})$ and effective interaction parameters Γ (see equation (3)) from neutron scattering experiments on mixtures of D-PMMA and PSAN-19 evaluated according to equation (5). $\langle \bar{N}\rangle_w$ calculated according to equation (6) with $\langle N_A^*\rangle_w = 2120$ (D-PMMA) and $\langle N_B^*\rangle_w = 2630$ (PSAN-19)

Mass fraction of D-PMMA, w	Volume fraction, Φ	Average polymerization degree, $\langle \bar{N}\rangle_w$	D17 measurements (after annealing at 140°C)		D11 measurements (after annealing at 140°C)		D17 measurements (after annealing at 200°C)	
			R_g(nm)	$-\Gamma(\times 10^3)$	R_g(nm)	$-\Gamma(\times 10^3)$	R_g(nm)	$-\Gamma(\times 10^3)$
0.05	0.042	2137	15.2	25.5	15.4	27.8		
0.10	0.085	2156	14.2	22.9	15.0	27.9	16.1	16.4
0.20	0.173	2194	13.2	25.2	13.0	26.4	16.1	14.9
0.30	0.264	2234	12.7	22.2	11.7	26.1	16.0	15.2
0.40	0.358	2278	12.2	20.5	11.7	22.2	15.8	13.5
0.50	0.455	2325	13.4	16.4	13.5	12.5	16.1	9.8
0.60	0.556	2376	14.5	13.0	14.4	15.0	16.7	9.6
0.70	0.661	2432	15.2	11.0	14.5	11.0	16.2	6.4
0.80	0.770	2492	16.1	7.7	16.1	7.4	16.4	4.7
0.90	0.883	2558			16.3	5.7	16.7	3.7

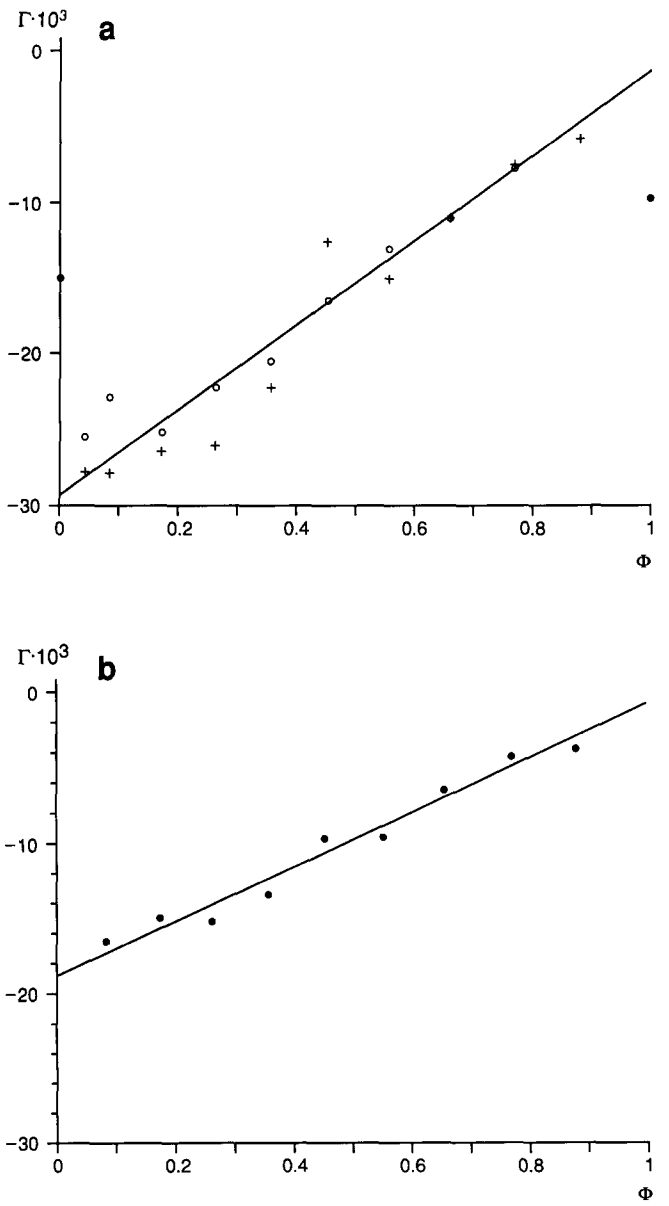

Figure 7 Effective interaction parameter Γ (equations (3a) and (b)) *versus* the volume fraction Φ of D-PMMA in mixtures of D-PMMA and PSAN-19. (a) Samples annealed at 140°C; ○, D17 instrument; +, D11 instrument; ●, data from refs 1 and 3 annealed at 130°C. (b) Samples annealed at 200°C; D17 instrument

Φ-Dependence of the effective Flory–Huggins parameter and the radius of gyration

Effective Flory–Huggins parameter. The Φ-dependence of the effective Flory–Huggins parameter Γ was determined for mixtures annealed at 140°C and 200°C. The 140°C samples were measured using the D11 and D17 diffractometers, while the 200°C samples were measured using the D17 diffractometer only. The preparation conditions of the different samples are listed in *Table 4*. The effective Flory–Huggins parameters were evaluated from the Zimm representations of the scattering intensities according to equation (9). They are compiled in *Table 7*, together with the average polymerization degrees $\langle \bar{N}(\Phi)\rangle_w$ used for this purpose, the latter being calculated according to equation (6).

The Γ-profiles obtained for both annealing temperatures are shown in *Figure 7*. As can be seen from this figure, the Γ-values of the 140°C samples obtained from measurements using different instruments are identical within experimental certainty. Negative Γ-parameters of very high magnitude ($|\Gamma(\Phi)| \gg 1/\langle \bar{N}(\Phi)\rangle_w$) are obtained over the whole Φ-range, indicating that the system D-PMMA/PSAN-19 is highly compatible. The effective Flory–Huggins parameters of the samples annealed at 200°C are significantly smaller than those of the samples annealed at 140°C.

The Γ-parameters measured in the dilute systems of D-PMMA in PSAN-19 and PSAN-19 in D-PMMA[3] for annealing temperatures of 130°C are also shown in *Figure 7a* ($\Gamma = -0.015$ and -0.0097, respectively). These data agree fairly well with $\Gamma(0)$ and $\Gamma(1)$ obtained from an extrapolation of the Γ-profile determined in the concentrated systems. The latter are more reliable due to the larger effects in the scattering intensity at higher concentrations.

In *Figures 7a* and *b* the solid lines represent linear fits of the experimental data. With the boundary condition $\Phi(1-\Phi)\chi(\Phi) = 0$ for $\Phi = 0$ and 1 it can be shown that $\chi(\Phi)$ is a polynomial of the same order as $\Gamma(\Phi)$ (see appendix B). Inserting the linear fits for $\Gamma(\Phi)$ in equation (3) the χ-profiles of *Figure 8* were determined. As can be seen from this figure, the χ-parameter increases with increasing volume fraction of D-PMMA for both annealing temperatures. For the higher annealing temperature the χ-parameters are of smaller magnitude irrespective of the composition of the mixture.

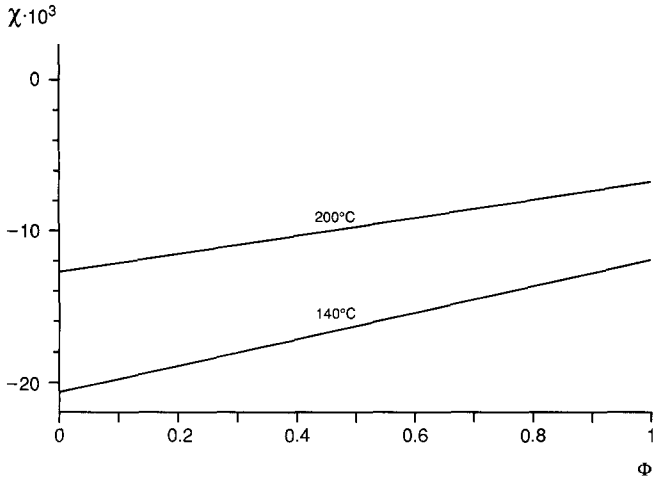

Figure 8 Flory–Huggins parameter χ (equation (3a)) *versus* the volume fraction Φ of D-PMMA in mixtures of D-PMMA and PSAN-19. The lines drawn for 140°C and 200°C were calculated according to equation (3b) from the lines in *Figures 7a* and *b*, respectively

Radii of gyration. The radii of gyration $R_g(=\langle\bar{R}_g^2\rangle_z^{1/2})$ determined from the Zimm representations of the mixtures of the three sample sets are listed in *Table 7*. This evaluation was performed according to equation (5) using $\langle\bar{N}\rangle_w$ as calculated with equation (6) and the experimentally determined Γ. In *Figure 9* the $\langle R_g(\Phi)\rangle$ profiles of the samples are represented. For comparison, the z-average radii of gyration determined in the bulk state[2,8] and the dilute mixtures[3] are also shown. The dashed lines represent the profile of the average radius of gyration $\langle\bar{R}_g\rangle_z$, according to equation (7). Note that both values on the ordinate are radii of PMMA molecules and that radii of PSAN-19 occur at Φ(D-PMMA)=1.

From *Figure 9a* it can be seen that the R_g profile of the concentrated mixtures annealed at 140°C shows a clear Φ-dependence with a pronounced minimum at about $\Phi=0.35$. Around this minimum the $\langle R_g\rangle_z$ values are smaller than those determined in the bulk state of both components. A similar small $\langle R_g\rangle_z$ value is not observed for the thermodynamically concentrated but optically dilute system (mixture with Φ(PMMA)=0.31, 1% of which deuterated). Within experimental certainties the radius of gyration of D-PMMA measured in the optically dilute system agrees with that determined in the bulk state. The radii of gyration $R_g(0)$ and $R_g(1)$ extrapolated from the R_g profile for Φ to 0 and 1 agree well with the values determined in the diluted systems.

As can be seen from *Figure 9b*, the R_g profiles of the mixtures annealed at 200°C do not show a significant Φ-dependence. Within the experimental certainties they agree with the radii of gyration expected from the measurements in the bulk state. There seems to be a trend to slightly lower R_g values in the middle Φ-range. For this sample set too, the extrapolated radii of gyration $R_g(0)$ and $R_g(1)$ are in good agreement with those determined in the dilute systems.

According to equation (12) a non-linear Φ-dependence of the apparent radius of gyration can be described with a Q-dependent Γ-parameter. If this view is adopted, from the difference between experimental points ($\langle\bar{R}_g^2\rangle_z$) and the dashed lines ($=\langle\bar{R}_g^2\rangle_z$) in *Figure 9* the quantity r_0^2 in equation (12) can be calculated.

However, the Φ-dependence of the radii of gyration could also reflect actual changes in the chain conformation. Such conformational changes could be caused, for example, by the influence of the intermolecular interactions on the rotational states of both chains. As will be discussed later, scattering data in the intermediate Q-range provide evidence that this is actually the case for the system under consideration.

Scattering data at intermediate Q-values

For a binary mixture of two 'Debye chains' with identical Schulz–Flory molecular mass distributions, the form factor $S(Q)$ at intermediate and high Q-values can be described to a good approximation by the quantities R_g and Γ, determined in the small-angle regime (see equation (17)). This means that the scattering data at intermediate Q-values can be used to check the validity of the evaluation procedure of the small-angle data.

Measurements at intermediate Q-values were carried out only for the sample set annealed at 140°C. In *Figures 10a* to *d* the scattering intensities are represented in the

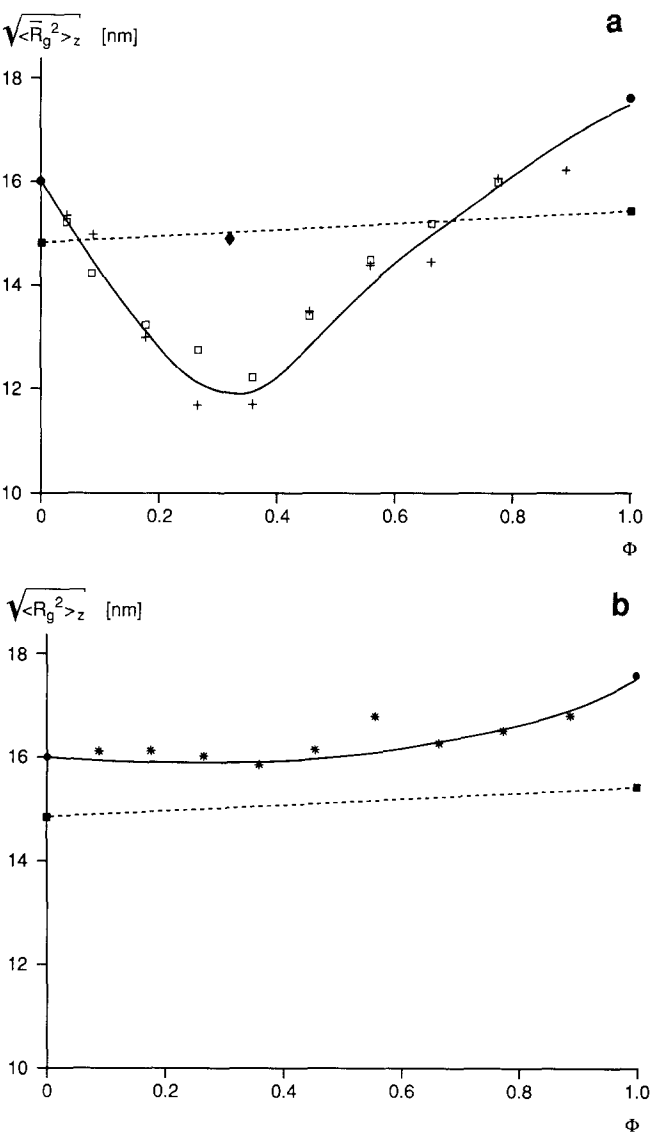

Figure 9 Radius of gyration $\sqrt{\langle\bar{R}_g^2\rangle_z}$ *versus* the volume fraction Φ of D-PMMA. Annealing temperature: (a) 140°C; (b) 200°C. Instrument used: □, *, D17; +, D11. ●, Values from dilute systems[3]; ■, bulk data[2,8]; ◆, optically thin (corresponds to ▽ in *Figure 6*). The relative error of $\sqrt{\langle\bar{R}_g^2\rangle_z}$ (important for the significance of the occurrence of a minimum, for example) is estimated to be ≤1 nm

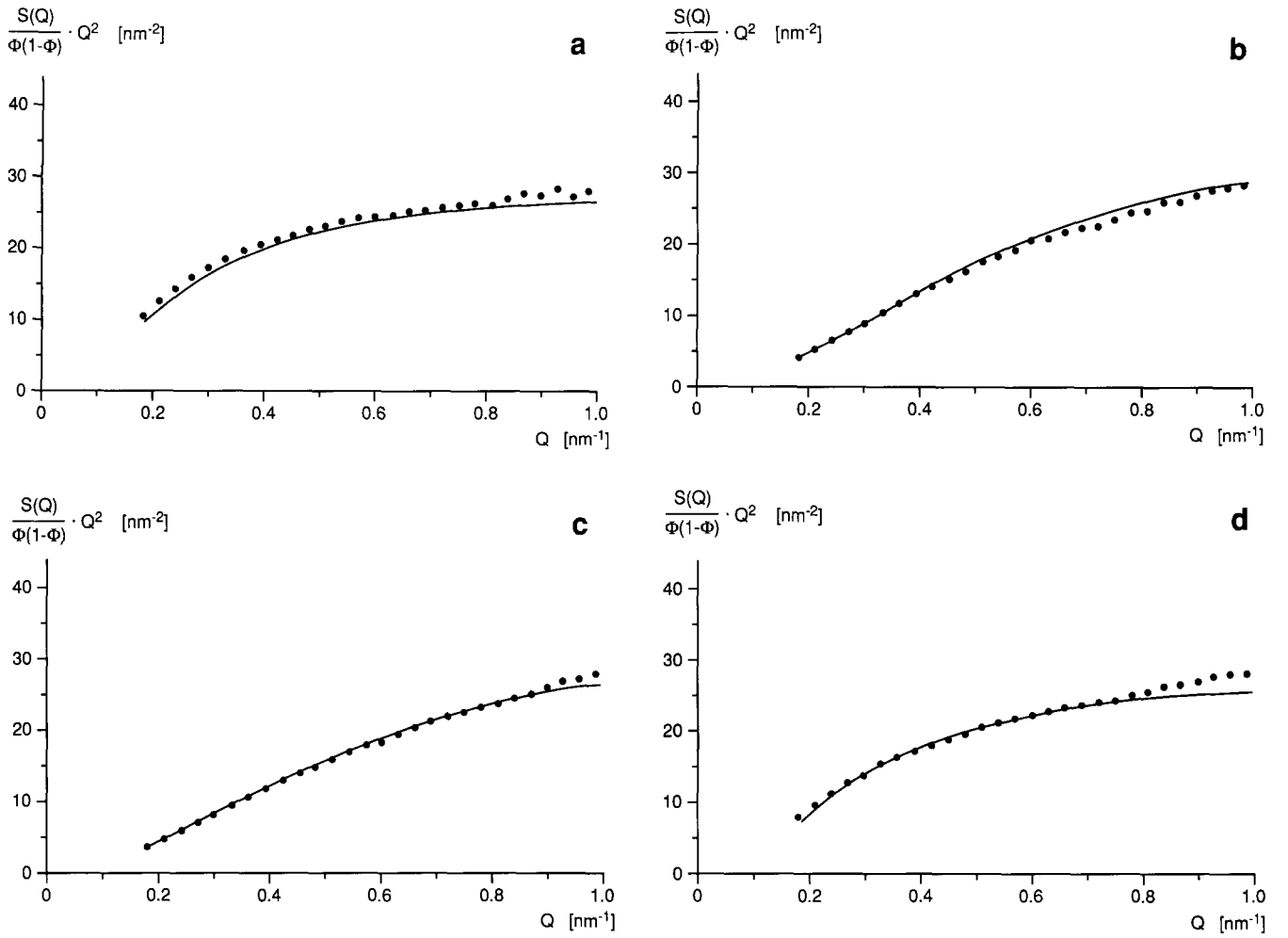

Figure 10 Kratky plot of SANS data at intermediate Q-values. Volume fractions Φ of D-PMMA: (a) 0.042; (b) 0.173; (c) 0.455; (d) 0.770. Drawn lines calculated according to equation (17) with $\langle \bar{R}_g^2 \rangle_z$ and Γ from $\lim_{Q \to 0}$ results

so-called Kratky form ($S(Q)Q^2/[\Phi(1-\Phi)]$ *versus* Q) for four different volume fractions of D-PMMA. The dashed lines are the intensity profiles calculated according to equation (17) using the $\langle \bar{N} \rangle_w(\Phi)$, the $R_g(\Phi)$ and $\Gamma(\Phi)$ values (D17 measurements), listed in *Table 7*. As can be seen, the small-angle data provide a reasonably good description of the experimental data at intermediate Q-values. The deviations observed at Q-values larger than $0.8\,nm^{-1}$ are most likely related to errors in the subtraction of the incoherent background. It should be mentioned that for $Q > 0.3\,nm^{-1}$ no deviations larger than 10% were observed for any of the samples investigated.

These results show that the evaluation method applied to the small-angle data — namely the dismissing of the scattering intensities at the smaller Q-values — results in R_g and Γ-values which allow a consistent description of the intermediate Q data. Furthermore they demonstrate that the scattering intensities at intermediate Q-values can be described with a Debye form factor for both chains. As already mentioned, neutron scattering data of PMMA in the bulk state deviate significantly from a Debye-like scattering behaviour, showing a maximum in the Kratky representation[8,30] at $Q \approx 0.5\,nm^{-1}$. A maximum at about the same Q-value was also found in mixtures of poly(ethylene oxide) and PMMA[31].

As can be seen from *Figure 10* the scattering data of the mixtures do not provide any evidence for the existence of a maximum in the Q-range investigated. To make sure that maxima (if they exist) are not suppressed by the large magnitudes of the interaction parameters $\Gamma(\Phi)$, a 'corrected' bulk structure factor was calculated for $\Phi = 0.042$ according to equation (18), where $\langle N_A^* \rangle_w P_A(Q) = \langle N_B^* \rangle_w P_B(Q) = \langle N^* \rangle_w P(Q)$ was inserted in equation (2):

$$\Phi(1-\Phi)/S_{corr}(Q) = [\langle N^* \rangle_w P(Q)]^{-1} - 2\Phi(1-\Phi)\Gamma(\Phi) \quad (18)$$

The PMMA structure factor measured in the bulk state[8] and $\Gamma(\Phi) = -0.0255$, as determined for the $\Phi = 0.042$ mixture (see *Table 7*) were inserted in equation (18) for $\langle N^* \rangle_w P(Q)$ and $\Gamma(0.042)$, respectively. As can be seen from *Figure 9* the PMMA chain extension in the bulk and in the $\Phi = 0.042$ mixture is the same within the limits of experimental certainty. Therefore one would expect the Kratky representations of the 'corrected' structure factor and the $\Phi = 0.042$ mixture to be the same, assuming that the PMMA chain has a 'Debye conformation' in both systems. As is discussed in ref. 4, the 'Kratky plateau' can be considered to be a measure of the average monomer density of a chain, i.e. it should depend on the chain's extension only. This conclusion is only slightly affected by the contributions of the PSAN-19 form factor to the measured structure factor of the $\Phi = 0.042$ mixture. As the chain extensions of D-PMMA and PSAN-19 are

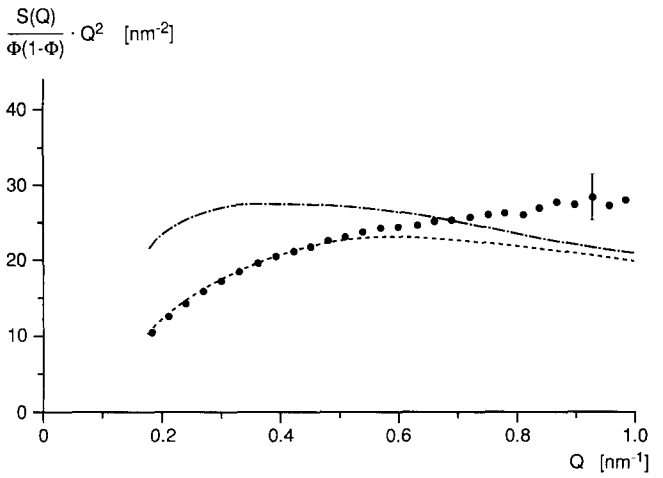

Figure 11 Kratky plot of SANS data. ●, Experimental values from *Figure 10a* (Φ of D-PMMA = 0.042); –·–·–, bulk data for PMMA[8]; – – – –, bulk data of PMMA 'corrected' for thermodynamic interaction according to equation (18)

not too different, deviations resulting from these contributions should be considerably smaller than 5%.

In *Figure 11* the Kratky profiles of the 'corrected' structure factor and the structure factors measured in the bulk state of PMMA and in the $\Phi = 0.042$ mixture are represented. As can be seen, the maximum in the scattering curve of the bulk data is considerably modified by the introduction of the interaction parameter $\Gamma(\Phi)$. For $Q < 0.5\,\mathrm{nm}^{-1}$ the 'corrected' structure factor of the bulk data is in excellent agreement with that of the structure factor of the $\Phi = 0.042$ mixture. As already mentioned, the accordance of the Kratky profiles at small Q-values simply reflects the fact that the PMMA chain has the same extension in both environments. For Q-values larger than $0.5\,\mathrm{nm}^{-1}$ the Kratky profiles of the 'corrected' bulk data and the $\Phi = 0.042$ mixture start to deviate from each other. Whereas the bulk data decrease, giving rise to a maximum at about $0.5\,\mathrm{nm}^{-1}$, the mixture data increase slightly over the entire Q-range.

The question arises as to whether this deviation indicates an actual difference in the local conformation of the PMMA chain in both environments or whether it is related to a systematic error in the subtraction of the incoherent background. As is indicated by the error bar in *Figure 11* the experimental errors of the mixture measurement cannot account for the differences in the structure factors. To investigate the influence of the incoherent background subtraction on the Kratky profile, the scattering data of the $\Phi = 0.042$ mixture were re-evaluated by subtracting an 'incoherent background' which was arbitrarily chosen to match the Kratky profiles of the mixture and the 'corrected' bulk data at large Q values. As can be seen from *Figure 12* this procedure leads to significant deviations in the Q-range from 0.4 to $0.7\,\mathrm{nm}^{-1}$, indicating that the differences in the corresponding Kratky profiles, shown in *Figure 11*, are most likely not related to an incorrect subtraction of the incoherent background.

This would mean that the local chain conformation of PMMA in the bulk state is different from its conformation in the concentrated mixtures of D-PMMA/PSAN-19. This, however, is in contradiction to the generally accepted assumption that the chain conformation is the same in the bulk and in concentrated mixtures. As mentioned earlier such conformational changes could be caused, for example, by the influence of the intermolecular interactions on the statistical weights of the rotational states of the chain molecules. That intermolecular interactions might actually have an influence on the chain conformation, despite excluded volume effects, can also be concluded from X-ray investigations of the chain conformation of PMMA dissolved in different low molecular mass solvents[30]. As can be seen from *Figure 13*, the Kratky representation of the scattered intensity shows a pronounced minimum at $Q = 2.5\,\mathrm{nm}^{-1}$ ($\vartheta = 3.5°$) for PMMA dissolved in a θ solvent. With increasing quality of the solvent this minimum flattens out significantly, so that for the best solvent investigated (benzene) the Kratky profile almost has the form of a plateau. The disappearance of the pronounced minimum for good solvents is in agreement with the observation that in the good, high molecular mass solvent PSAN-19, the PMMA form factor does not show a maximum either.

In the framework of this picture it may be imagined that the chain conformation also changes with the composition and the thermal treatment of the mixtures.

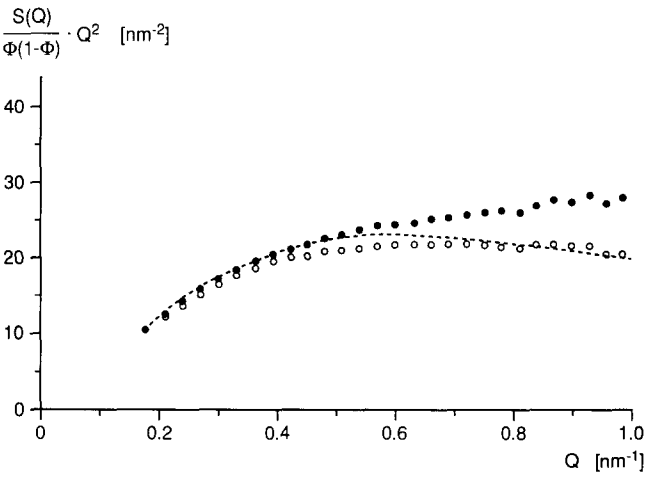

Figure 12 Kratky plot of SANS data. ●, experimental data and – – – –, 'corrected' bulk data, both from *Figure 11*. ○, Experimental data subtracting a background, chosen to fit with the 'corrected' bulk data at $Q = 1\,\mathrm{nm}^{-1}$

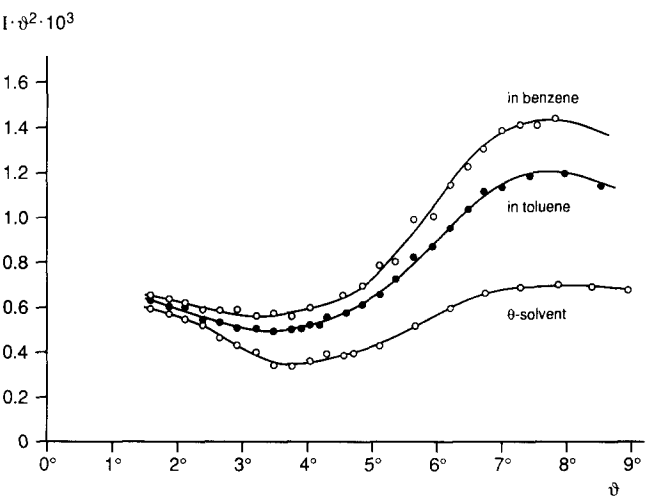

Figure 13 Kratky plot of small-angle X-ray scattering data on PMMA solutions in solvents of different quality[30]. The θ-solvent is a mixture of butanone and isopropanol. $\lambda = 0.154\,\mathrm{nm}$

This would mean that the Φ-dependence of the radius of gyration of the 140°C samples does not necessarily indicate a Q-dependence of the Γ-parameter. It could also be due to changes in the actual conformations of the chains.

However, it has to be stressed that this hypothesis is speculative as long as there is no clear proof that the chain conformation in the bulk and in the concentrated mixtures is really different. In order to obtain the necessary information, measurements at Q-values larger than $1\,nm^{-1}$ have to be carried out. In this Q-range possible differences in the local conformations of the chain molecules can be detected. However, on conventional diffractometers, such as the D17, these measurements suffer from the uncertainties in the subtraction of the incoherent background. Therefore the 'wide angle' measurements will have to be carried out on a diffractometer with spin analysis capabilities which allow experimental determination of the incoherent background[32].

REFERENCES

1 Kruse, W. A., Kirste, R. G., Haas, J., Schmitt, B. J. and Stein, D. J. *Makromol. Chem.* 1976, **177**, 1145
2 Schmitt, B. J., Kirste, R. G. and Jelenič, J. *Makromol. Chem.* 1980, **181**, 1655
3 Jelenič, J., Kirste, R. G., Oberthür, R. C., Schmitt-Strecker, S. and Schmitt, B. J. *Makromol. Chem.* 1984, **185**, 129
4 de Gennes, P. G. 'Scaling Concepts in Polymer Physics', Cornell University Press, Ithaca, 1979
5 Joanny, J. F. *C.R. Acad. Sci., Paris* 1978, **286B**, 89
6 Schwahn, D., Mortensen, K., Springer, T., Yee-Madeira, H. and Thomas, R. *J. Chem. Phys.* 1987, **87**, 6078
7 Binder, K. *J. Chem. Phys.* 1983, **79**, 6387
8 Kirste, R. G., Kruse, W. A. and Ibel, K. *Polymer* 1975, **16**, 120
9 Yoon, D. Y. and Flory, P. J. *Polymer* 1975, **16**, 645
10 Greschner, G. S. *Makromol. Chem.* 1973, **170**, 203
11 Kirschey, M. PhD Dissertation, Johannes Gutenberg Universität, Mainz, 1989
12 Jelenič, J. PhD Dissertation, Johannes Gutenberg Universität, Mainz, 1979
13 Kruse, W. A. PhD Dissertation, Johannes Gutenberg Universität, Mainz, 1974
14 Elias, H.-G. 'Makromoleküle', 4th Edn, Hüthig & Wepf Verlag, Basel, 1975
15 Ferguson, R. C. and Ovenall, D. W., *Macromolecules* 1987, **20**, 1245
16 Blank, H. and Maier, B. 'The Yellow Book: Guide to Neutron Research Facilities at the ILL', Grenoble, 1988
17 Ibel, K. *J. Appl. Cryst.* 1976, **9**, 296
18 Gosh, R. ILL Report 81 GH 29 T, Grenoble, France, 1981
19 Jacrot, B. and Zaccai, G. *Biopolymers* 1981, **20**, 2413
20 Ohm, H. PhD Dissertation, Johannes Gutenberg Universität, Mainz, 1985
21 Hayashi, H., Flory, P. J. and Wignall, G. D. *Macromolecules* 1983, **16**, 1328
22 O'Reilly, J. M., Teegarden, D. M. and Wignall, G. D. *Macromolecules* 1985, **18**, 2747
23 Gawrisch, W., Brereton, M. G. and Fischer, E. W. *Polym. Bull.* 1981, **4**, 687
24 Akcasu, A. Z., Summerfield, G. C., Jahshan, S. N., Han, C. C., Kim, C. Y. and Yu, H. J. *J. Polym. Sci., Polym. Phys. Edn* 1980, **18**, 863
25 Braun, H. G. BASF AG, personal communication, 1988
26 Koberstein, J. T., Picot, C. and Benoit, H. *Polymer* 1985, **26**, 673
27 Wendt, E. and Springer, J. *Polymer* 1988, **29**, 1301
28 Dautzenberg, H. *J. Polym. Sci., Polym. Phys. Edn* 1977, **61**, 83
29 Oberthür, R. C. *Makromol. Chem.* 1978, **179**, 2693
30 Wunderlich, W. and Kirste, R. G. *Ber. Bunseng. Physik. Chem.* 1964, **68**, 646
31 Lefebvre, J.-H. R., Porter, R. S. and Wignall, G. D. *Polym. Eng. Sci.* 1987, **27**, 433
32 Schärpf, O. ILL, Grenoble, personal communication, 1988
33 Guinier, A. 'X-ray Diffraction', W. H. Freeman, San Francisco, 1963

APPENDIX A

Subtraction of the coherent background

We will assume that the coherent background is due to inclusion of particles such as solvent residues, catalyst residues or voids. No contributions due to density fluctuations are taken into account. It will further be assumed that the particle density of the sample containing inclusions can be derived from the particle density of an inclusion-free sample by means of a mask function $V(\vec{X})$, defined as:

$$V(\vec{X})=\begin{cases}0 & \text{if a monomer unit occupies lattice site } \vec{X}\\ 1 & \text{if an inclusion particle occupies lattice site } \vec{X}\end{cases}$$

and

$$1/V\int V(\vec{X})\,d\vec{X}=\mu$$

where μ is the volume fraction of the inclusions (V = scattering volume).

The description of the inclusions by means of a mask function means that no interfacial effects, such as a change of the chain conformation in the interface area, are taken into account.

With the mask function $V(\vec{X})$ the particle density $\varrho(\vec{X})$ of the sample containing inclusions can be written:

$$\varrho(\vec{X})=\varrho_f(\vec{X})-\varrho_f(\vec{X})V(\vec{X})+\varrho_V V(\vec{X}) \qquad (A1)$$

where $\varrho_f(\vec{X})$ is the particle density of the inclusion-free sample and ϱ_V is the homogeneous particle density of the inclusions.

In the lattice model the particle density $\varrho_f(\vec{X})$ of a binary incompressible mixture can be written:

$$\varrho_f(\vec{X})=v_0^{-1}\left[\frac{v_0}{v_A}\Phi_A(\vec{X})+\frac{v_0}{v_B}\Phi_B(\vec{X})\right] \qquad (A2)$$

where $\Phi_A(\vec{X})$ and $\Phi_B(\vec{X})$ are dimensionless density functions defined in the Theoretical Background section. v_A and v_B are the monomer volumes of both components and v_0 is the volume of a lattice cell. The density functions $\Phi_A(\vec{X})$ and $\Phi_B(\vec{X})$ can be written in the form:

$$\Phi_A(\vec{X})=\Phi+\Delta\Phi_A(\vec{X}); \qquad \Phi_B(\vec{X})=(1-\Phi)+\Delta\Phi_B(\vec{X})$$

where Φ and $(1-\Phi)$ are the average values of $\Phi_A(\vec{X})$ and $\Phi_B(\vec{X})$ and $\Delta\Phi_A(\vec{X})$ and $\Delta\Phi_B(\vec{X})$ are the local deviations from these mean values. According to the incompressibility condition $\Delta\Phi_A(\vec{X})=-\Delta\Phi_B(\vec{X})=\Delta\Phi_f(\vec{X})$. That means $\varrho_f(\vec{X})$ can be rewritten:

$$\varrho_f(\vec{X})=v_0^{-1}\left\{\left[\Phi\frac{v_0}{v_A}+(1-\Phi)\frac{v_0}{v_B}\right]+\left(\frac{v_0}{v_A}-\frac{v_0}{v_B}\right)\Delta\Phi_f(\vec{X})\right\} \qquad (A3)$$

From equation (A3) one obtains for the scattering amplitude[33] of the inclusion-free samples:

$$A_f(\vec{Q})=v_0^{-1}\left[\Phi b_A\frac{v_0}{v_A}+(1-\Phi)b_B\frac{v_0}{v_B}\right]\delta(\vec{Q})+v_0^{-1}\left(b_A\frac{v_0}{v_A}-b_B\frac{v_0}{v_B}\right)\Delta\Phi_f(\vec{Q}) \qquad (A4)$$

with the delta function $\delta(\vec{Q})=\int\exp(i\vec{Q}\vec{X})\,d\vec{X}$ and the Fourier transform of $\Delta\Phi_f(\vec{X})$:

$$\Delta\Phi_f(\vec{Q})=\int\Delta\Phi_f(\vec{X})\exp(i\vec{Q}\vec{X})\,d\vec{X}$$

Note that for $\vec{Q} \neq 0$ the differential cross-section per unit volume of a homogeneous binary mixture can be written:

$$\frac{d\Sigma}{d\Omega}(Q) = 1/V\langle A_f(\vec{Q})A_f(-Q)\rangle = V^{-1}v_0^{-2} \times \left(b_A\frac{v_0}{v_A} - b_B\frac{v_0}{v_B}\right)^2 \langle \Delta\Phi_f(\vec{Q})\Delta\Phi_f(-\vec{Q})\rangle \quad (A5)$$

where V is the scattering volume containing N lattice sites. The angular brackets denote a thermal and spatial averaging. The dimensionless quantity $v_0^{-2}\langle \Delta\Phi_f(\vec{Q})\Delta\Phi_f(-\vec{Q})\rangle$ can be considered to be the scattering power of these N lattice sites. Therefore the scattering power $S(Q)$ per lattice site is given by:

$$S(Q) = N^{-1}v_0^{-2}\langle \Delta\Phi_f(\vec{Q})\Delta\Phi_f(-\vec{Q})\rangle \quad (A6)$$

Inserting equation (A6) into equation (A5) one obtains the following equation for the differential cross-section per unit volume of a binary incompressible mixture not containing any inclusions (see equations (1a) and (1b)):

$$\frac{d\Sigma}{d\Omega_f}(Q) = v_0^{-1}\left(b_A\frac{v_0}{v_A} - b_B\frac{v_0}{v_B}\right)^2 S(Q) = v_0\left(\frac{b_A}{v_A} - \frac{b_B}{v_B}\right)^2 S(Q) \quad (A7)$$

where $S(Q)$ for a binary mixture in the mean field random phase approximation is given by equation (2).

The scattering amplitude for a system containing inclusions can be derived from the density function of equation (A1):

$$A(\vec{Q}) = A_f(\vec{Q}) - A_f(\vec{Q})*V(\vec{Q}) + b_V\varrho_V V(\vec{Q}) \quad (A8)$$

where * denotes the faltung product defined as

$$A_f(Q)*V(Q) = \int A(\vec{U})V(\vec{Q}-\vec{U})\,d\vec{U}$$

With $\delta(\vec{Q})*V(\vec{Q}) = V(\vec{Q})$ one obtains:

$$A_f(\vec{Q})*V(\vec{Q}) = v_0^{-1}\left\{\left[\Phi b_A\frac{v_0}{v_A} + (1-\Phi)b_B\frac{v_0}{v_B}\right]V(\vec{Q}) + \left(b_A\frac{v_0}{v_A} - b_B\frac{v_0}{v_B}\right)\Delta\Phi_f(\vec{Q})*V(\vec{Q})\right\}$$

Inserting this expression into equation (A8) yields:

$$A(\vec{Q}) = A_f(\vec{Q}) - v_0^{-1}\left\{\left[\Phi\left(b_A\frac{v_0}{v_A} - b_V\frac{v_0}{v_V}\right) + (1-\Phi)\left(b_B\frac{v_0}{v_B} - b_V\frac{v_0}{v_V}\right)\right]V(\vec{Q}) + \left(b_A\frac{v_0}{v_A} - b_B\frac{v_0}{v_B}\right)\Delta\Phi_f(\vec{Q})*V(\vec{Q})\right\} \quad (A9)$$

Inserting the scattering amplitude:

$$A_{A/B}(\vec{Q}) = v_0^{-1}\left(b_V\frac{v_0}{v_V} - b_{A/B}\frac{v_0}{v_{A/B}}\right)V(\vec{Q})$$

of the inclusion-free blank samples ($\Delta\Phi_f^{A/B}(\vec{Q}) = 0$ according to the incompressibility assumption) into equation (A9) one obtains:

$$A(\vec{Q}) = A_f(\vec{Q}) - [\Phi A_A(\vec{Q}) + (1-\Phi)A_B(\vec{Q})] - v_0^{-1}\left(b_A\frac{v_0}{v_A} - b_B\frac{v_0}{v_B}\right)\Delta\Phi_f(\vec{Q})*V(\vec{Q}) \quad (A10)$$

where we have assumed that $V(\vec{Q})$ is the same for the blank samples and the mixtures.

As expected, relation (A10) shows that generally the contribution of the faltung product to the coherent background cannot be corrected by subtracting the scattering contributions of the blank samples. Only in the special case of very large inclusions (significantly larger than the extension of the chain molecules) does the situation become simple again. Then $V(\vec{Q})$ has the form of a relatively sharp peak around $\vec{Q} = 0$ and the faltung product can be replaced to a good approximation by the product $\int V(\vec{Q})d(\vec{Q})\Delta\Phi_f(\vec{Q}) = \mu\Delta\Phi_f(\vec{Q})$.

Using this approximation the scattering amplitude for $\vec{Q} \neq 0$ can be written:

$$A(\vec{Q}) = (1-\mu)v_0^{-1}\left(b_A\frac{v_0}{v_A} - b_B\frac{v_0}{v_B}\right)\Delta\Phi_f(\vec{Q}) - v_0^{-1}\left\{\Phi\left(b_A\frac{v_0}{v_A} - b_V\frac{v_0}{v_V}\right) + (1-\Phi)\left(b_B\frac{v_0}{v_B} - b_V\frac{v_0}{v_V}\right)\right\}V(\vec{Q}) \quad (A11)$$

As can be seen from equation (A11) the effect of the inclusions in this case is to reduce the magnitude of the scattered amplitude of the inclusion-free mixture by the volume fraction μ of scattering volume occupied by the inclusions.

For the differential cross-section one obtains:

$$\frac{d\Sigma}{d\Omega}(Q) = (1-\mu)^2 v_0\left(\frac{b_A}{v_A} - \frac{b_B}{v_B}\right)^2 S(Q) + (Vv_0^2)^{-1} \times \left[\Phi b_A\frac{v_0}{v_A} + (1-\Phi)b_B\frac{v_0}{v_B} - b_V\frac{v_0}{v_V}\right]^2 \times \langle V(\vec{Q})V(-\vec{Q})\rangle \quad (A12)$$

Notice that the cross-term $\langle \Delta\Phi_f(\vec{Q})V(-\vec{Q})\rangle$ vanishes for $\vec{Q} \neq 0$ as the locations of the inclusions are not correlated to the locations of the chain molecules in the inclusion-free sample.

With the differential cross-sections of the blank samples:

$$\frac{d\Sigma}{d\Omega}(Q)_{A/B} = (Vv_0^2)^{-1}\left(b_{A/B}\frac{v_0}{v_{A/B}} - b_V\frac{v_0}{v_V}\right)^2 \langle V(\vec{Q})V(-\vec{Q})\rangle$$

equation (A12) can be written as:

$$\frac{d\Sigma}{d\Omega}(Q) = (1-\mu)^2 v_0\left(\frac{b_A}{v_A} - \frac{b_B}{v_B}\right)^2 S(Q) + \left[\Phi\left(\frac{d\Sigma}{d\Omega}(Q)_A\right)^{1/2} + (1-\Phi)\left(\frac{d\Sigma}{d\Omega}(Q)_B\right)^{1/2}\right]^2 \quad (A13)$$

as was assumed in the treatment of the coherent background subtraction described in the Experimental part. On the other hand the term $(1-\mu)^2$ is not taken into consideration in this procedure. As the volume fraction μ of inclusions is normally very small ($\mu \ll 1$) this effect should be negligible in most cases.

It should be mentioned that the faltung product cannot be responsible for the 'excess' scattering contributions observed in some of the mixtures. As can be seen from equation (A9) this term is independent of the volume

fraction Φ and therefore it should be the same for all mixtures, in contradiction to the experimental results.

APPENDIX B

For Γ a linear polynomial is assumed:

$$\Gamma = a_0 + a_1\Phi \tag{B1}$$

Then according to equation (3b)

$$\Phi(1-\Phi)\chi(\Phi) = -a_0\Phi^2 - \frac{a_1}{3}\Phi^3 + C_1\Phi + C_2 \tag{B2}$$

is obtained. C_1 and C_2 are the integration constants. From the boundary condition $\Phi(1-\Phi)\chi(\Phi)=0$ at $\Phi=0$ and $\Phi=1$ one obtains $C_2=0$ and $C_1=a_0+(a_1/3)$. This yields:

$$\chi(\Phi) = g_0 + g_1\Phi \quad \text{with} \quad g_0 = a_0 + \frac{a_1}{3} \quad \text{and} \quad g_1 = \frac{a_1}{3} \tag{B3}$$